Influence of Zeolite Framework Geometry Structure on the Stability of the $[ZnOZn]^{2+}$ Cluster by Periodical Density Functional Theory

Luis Antonio M. M. Barbosa* and Rutger A. van Santen

Schuit Institute of Catalysis, Eindhoven University of Technology, P.O. Box 513, 5600 MB Eindhoven, The Netherlands

Received: November 7, 2002; In Final Form: February 27, 2003

The location of the $[ZnOZn]^{2+}$ cluster in zeolites has been studied by the periodical density functional method for a chosen composition of two Si atoms substituted by two Al atoms in the same D6R unit cell of the chabazite framework. This leads to different arrangements for Al pair in two ring configurations: six- and eight-membered. The cationic cluster is most stabilized when placed in the eight-membered ring. There are two factors playing a major role in the stabilization of this site: the accommodation of framework stress and the electrostatic interaction provided by the oxygen atoms of the framework. In the case of the six-membered ring, the stability is markedly influenced by the electrostatic interaction due to the close proximity of the Zn cations to the ring plane. On the other hand, both factors are important for the stability of the $[ZnOZn]^{2+}$ site in eight-membered rings. However, accommodation of the framework stress seems to be the main factor for the different stabilization results within the eight-membered family.

1. Introduction

In many industrial processes, zeolites are employed as a solid acidic catalysts. This chemical behavior is achieved due to the substitution of Si^{+4} by Al^{+3} cations in the zeolite framework, which creates an excess of negative charge in the framework. This negative charge needs to be compensated by addition of countercations. If they are protons, Brønsted acid sites are formed. On the other hand, if metallic cations are used, Lewis acid sites are created.

One example of a Lewis acid catalyst is the Zn^{+2} exchanged zeolites. In this case, two Brønsted acid sites have been substituted by one Lewis acid site. This catalyst is well-known for promoting the alkane aromatization reaction.[1−5] Currently, other chemical reactions have been shown to be promoted by this catalyst, such as nitrile hydrolysis,[6] sulfonation of substituted benzenes,[7] and ammination of triple bonds.[8]

In the alkane aromatization process the zeolite typically employed is ZnHZSM-5, which has a low aluminum content. Consequently, two Brønsted acid sites are unlikely to be in the same neighborhood. Many experimental studies have been focused on the understanding of what is the actual active site in this type of catalyst.[3,9−13]

One interesting proposal is the formation of $[ZnOZn]^{2+}$ species.[1,3] This type of species has been initially suggested for other divalent cations such as Fe and Cu.[14−16] In a previous study, calculations have shown that the $[ZnOZn]^{2+}$ site is more favorable when ZnO particles are employed to prepare Zn^{+2}-exchanged zeolites.[17]

To model the interaction between the cationic cluster and the zeolite framework, a cluster approach has been employed. The following systems have been studied: a 5T membered cluster[17,18] modeling part of the 10-membered ring of ZSM-5 and two interconnected five-membered rings[19] modeling the ZSM-5 framework.

Although the latter studies provide good insights on the local interaction between the $[ZnOZn]^{2+}$ species and the framework, these models are limited to a small portion of the entire zeolite framework. Thus a more detailed picture of the effect of the zeolite environment in the stability of this species is still needed.

The present work investigates systematically the stability of the $[ZnOZn]^{2+}$ site with the periodical density functional theory approach. The local distortions suffered by the zeolite structure upon $[ZnOZn]^{2+}$ formation and the effect of Al atom distribution within the zeolite ring structure on the stability of this site have been analyzed here.

2. Methods

In the work reported here all calculations were performed using the Vienna Ab initio Simulation Package (VASP).[20,21] This code carries out a periodic density functional calculations (DFT) using pseudopotentials and a plane wave basis set. The DFT was parametrized in the local-density approximation (LDA) with the exchange−correlation functional proposed by Perdew and Zunger[22] and corrected for nonlocality in the generalized gradient approximations (GGA) using the Perdew-Wang 91 functional.[23]

The interaction between the core and electrons is described using the ultrasoft pseudopotentials (US-PP) introduced by Vanderbilt[24] and provided by Kresse and Hafner.[25] The plane wave cutoff used here was 400.0 eV, which better describes the oxygen atom and all optimizations have been performed at the Γ point of the Brillouin zone. The structural parameters were considered to be converged at a constant volume and using a quasi-Newton algorithm if the forces on all atoms became smaller than 0.04 $eV\text{Å}^{-1}$.

* Corresponding author. Present address: Wilton Centre R-337, Wilton, Redcar, Cleveland, U.K. E-mail address:luis.barbosa@ici.com.

10.1021/jp022384g CCC: $25.00
Published on Web 04/17/2003

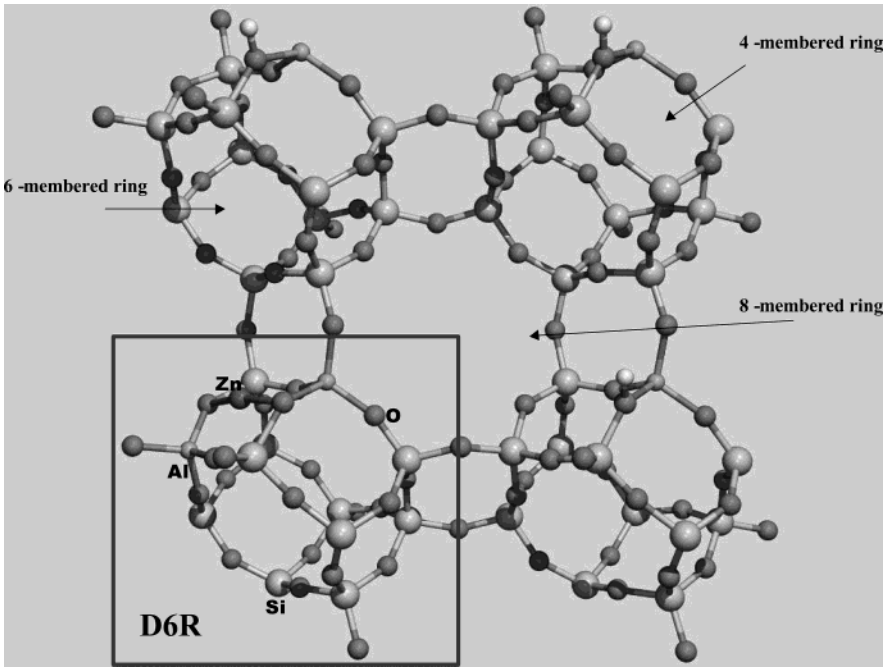

Figure 1. Chabazite structure with its unit cell.

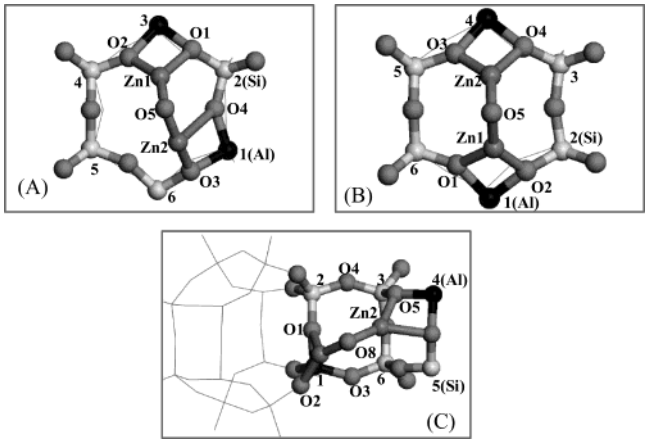

Figure 2. Six-membered ring configurations.

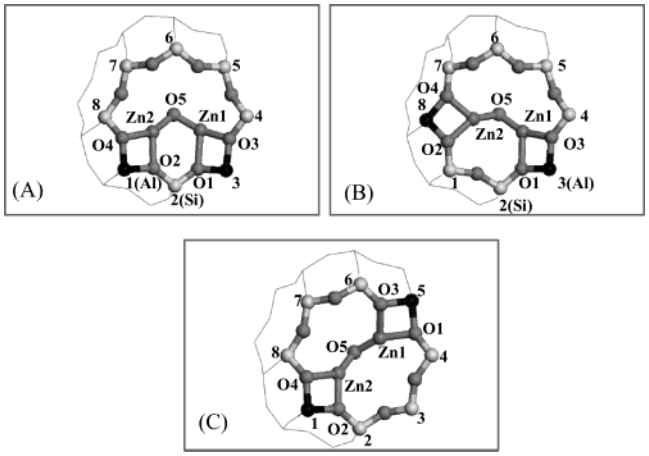

Figure 3. Eight-membered ring configurations.

To reduce the problems related to the residual stress, which appear due to variations of the unit cell volume, an optimization of the cell parameters has been followed. Details about this procedure can be found in elsewhere.[26,27]

The chabazite framework was chosen as a zeolite model because the unit cell contains only 12 TO_2 units, leading to less expensive calculations. This zeolite can be prepared with diverse Si/Al ratios and has micropores formed by eight-membered ring and cavities composed by four- and six-membered rings; see Figure 1.

The original model consists of one unit cell of chabazite (rhombohedrall cel, $a = 9.389$ Å and $\alpha = 94.33°$) as used previously by different authors.[26,28,29]

Two framework silicon atoms were replaced by two aluminum ones into the framework within the same unit cell. The ratio Si/Al = 5.0 is maintained constant in all cases. All different configurations obey Löwenstein's rule.[30]

The $[ZnOZn]^{2+}$ species have been placed in the different ring positions: 6T and 8T; see Figures 2 and 3. An extra six-membered ring position has also been analyzed, which corresponds to the connection of two 4T rings. In this case, each Al atom belongs to a different 4T ring.

Each ring type has been studied with a different Al atom distribution. All configurations are described by the number of Si atoms placed between two Al atoms. For instance, the six-membered ring is represented here by two different configurations: position 02 (AlSiAl) and 03 (AlSiSiAl); see Figure 2, parts a and b. The other six-membered ring (2×4T ring) is identified as position 04 (AlSiSiAl) (see Figure 2, part c). The eight-membered ring has three different possibilities, as seen in Figure 3, and represented by position 05 (AlSiAl), position 05 (AlSiSiAl), and position 05 (AlSiSiSiAl).

3. Results and Discussion

3.1. Preferred Location of $[ZnOZn]^{2+}$ Species. Usually Zn-zeolites are obtained, experimentally, by cationic exchange from protonic zeolites. Thus, the $[ZnOZn]^{2+}$ species is expected to be formed initially where Brønsted acids are least stable.

This should occur on large rings, viz., six- and eight-membered rings in the case of Chabazite. The former being more stable than the latter ones, as demonstrated previously for the Zn^{2+} cation case.[26] There are, however, special situations for the six-membered case, for instance, when it is formed by the interconnection of two four-membered rings (position 04).

TABLE 1: Energy Values for Stability of the Different $[ZnOZn]^{2+}$ Sites

type of zeolite site	formation energy[b]	absolute energy of the site[b]
six-membered ring		
position 02 (AlSiAl)	0.0	0.0
position 03 (AlSiSiAl)	−20	−28
position 04 (AlSiSiAl)	−10	−20
eight-membered ring		
position 05 (AlSiAl)	−37	−48
position 05 (AlSiSiAl)	−37	−32
position 05 (AlSiSiSiAl)	−42	−68

[a] All values in kJ/mol. [b] Referred to position 02.

SCHEME 1

$$2H^+ \text{ Zeolite} + 2\ ZnO \longrightarrow [ZnOZn]^{2+}\text{Zeolite} + H_2O$$

In this case, although both Brønsted sites behave as located in independent four-membered rings, this site behaves as a six-membered ring regarding the stability of the Zn^{2+} cation.

To verify the stability trend for the $[ZnOZn]^{2+}$ cluster, the formation energy of its corresponding site has been evaluated here by calculating the reaction energy of the process described by Scheme 1 and according to eq 1:

$$\Delta E_{(\text{position}-n)} = E([ZnOZn]^{2+}\text{Zeol})_{(\text{position}-n)} - E(H^+\text{Zeol})_{(\text{position}-n)} \quad (1)$$

The term $E(H^+\text{Zeol})_{(\text{position}-n)}$ represents the energy of a protonic zeolite with two Brønsted sites. All formation energy values are shown in Table 1. To compare the different results, they have been referred to the energy calculated for the position 02.

As a general trend, the $[ZnOZn]^{2+}$ species is more stable on the eight-membered ring. The same stability trend is observed if one compares rings with the same Al distribution. For instance, position 02 is less stable than position 05(AlSiAl) and position 03 is less stable than position 05 (AlSiSiAl).

The position 04 behaves as a six-membered ring. The formation energy is quite close to the one found for position 03, which has the same Al distribution. This confirms the previous trend, observed for the Zn^{2+} site's stability. However, the ring type stability trend has not been seen here: that of the eight-membered < that of the six-membered ring.

It is tempting to suggest that $[ZnOZn]^{2+}$ species' stability increases with the ring size. However, another factor may play a major role, which is the distance between both Al atoms. In very large rings (for instance 12-membered ring of Modernite), this could prevent the formation of this species. Nevertheless, it seems that the ring size has, indeed, some influence in the stability of this species.

3.2. Influence of Al Distribution on the Stability of $[ZnOZn]^{2+}$ Species. The energy of the site formation is biased by the stability of the parent Brønsted site pair. If one wants to verify the absolute stability of this site, it is necessary to decouple this influence. To do this, one needs to compare directly the absolute energy of the system ($E([ZnOZn]^{2+})$). These values are also found in Table 1 and again referred to the position 02.

A similar general trend for the stability is observed. However some new features start to emerge. The eight-membered ring positions have very similar formation energy values. This trend changes when one compares the absolute energies of these sites: position 05 (AlSiSiSiAl) > position 05 (AlSiAl) > position 05 (AlSiSiAl). Moreover, the $[ZnOZn]^{2+}$ species has a similar stability in both position 03 and position 05 (AlSiSiAl). This interesting result confirms the strong influence of the starting zeolite material has in the site population and the reactivity of Zn-exchanged zeolite.

TABLE 2: Results for the Optimized Geometry for the Different Six-Membered Rings

Al distribution active site	position 02 AlSiAl		position 03 AlSiSiAl		position 04 AlSiSiAl	
	H^+	$[ZnOZn]^{+2}$	H^+	$[ZnOZn]^{+2}$	H^+	$[ZnOZn]^{+2}$
T(1)−O−T(2)	145.0	147.3	141.1	139.5	134.2	138.9
T(2)−O−T(3)	135.5	138.3	160.7	161.2	153.5	145.2
T(3)−O−T(4)	147.5	139.6	136.0	136.5	132.7	134.5
T(4)−O−T(5)	148.0	151.0	142.7	139.5	157.9	142.0
T(5)−O−T(6)	151.5	150.3	151.1	149.8	138.2	142.0
T(6)−O−T(1)	136.2	136.2	139.0	141.9	155.2	143.5
T(6)−O−T(3)					143.7	133.6
Zn(1)−O(1)		2.04		2.05		2.14
Zn(1)−O(2)		1.99		1.99		1.96
Zn(1)−O(3)						3.25
Zn(2)−O(3)		1.88		2.01		
Zn(2)−O(4)		2.73		2.02		
Zn(1)−O(5)		1.81		1.79		
Zn(2)−O(5)		1.76		1.79		2.00
Zn(2)−O(6)						2.23
Zn(2)−O(7)						2.52
Zn(1)−O(8)						1.79
Zn(1)−O(8)						1.80

[a] Distances are in angstroms and angles in degrees.

It is clear that the stability of the $[ZnOZn]^{2+}$ species does not only depend on the ring size but also on Al distribution within the ring, which will be explored in detail in the following parts.

3.2.1. Six-Membered Ring Family. As shown previously, this family corresponds to positions 02, 03, and 04. The $[ZnOZn]^{2+}$ species at position 02 is the least stable configuration. Surprisingly, this has not been observed for the case of Zn^{+2} cation,[26] where this cation is found equally stable in both six-membered positions 02 and 03, with a slightly preference for the latter. The reason for the favored Zn(II) stability is the larger flexibility of the six-membered ring that allows for the distribution of the tension, created by the large ring distortions upon Zn(II) exchange, by adjusting the T−O−T angles.

The changes that occur in the T−O−T angles before and after the $[ZnOZn]^{2+}$ formation are 3 and 8° for position 03 and position 02, respectively (Table 2). These values are smaller than those found previously for the Zn^{2+} case. This different behavior comes from the relative position of the $[ZnOZn]^{2+}$ site, which is out of the plane of the framework oxygen atoms. Therefore, the flexibility of the six-membered ring does not play an important role for the stability of the $[ZnOZn]^{2+}$ site on this ring.

The Zn−O distances of the Zn cations to the framework oxygen atoms, however, show a possible trend. Both Zn cations have similar interaction with these atoms at position 03 (Table 2). The average value for the Zn−O distance in this case is 2.02 Å. On the other hand, there is an unbalanced interaction between the Zn cations and the six-membered ring at position 02, which leads to a higher average value for the Zn−O distance: 2.16 Å (see entries Zn(2)−O(2) and Zn(2)−O(4) in Table 2). This unbalanced interaction has been also observed from the Zn−O bond lengths of the bridge oxygen atom. This shows that the Zn(II) cations are closer to the ring plane, interacting better to the framework oxygen atoms at position 03.

Rozanska and collaborators[31] demonstrated that the electron density of the zeolite ring is shared among all oxygen atoms of

the ring with a slightly large contribution on the ones bond to the Al atom. The closer the cation is to the oxygen atoms, the better the electrostatic interaction. This explains the trend found for the six-membered family; the $[ZnOZn]^{2+}$ site is better stabilized at the position 03.

Although position 04 behaves as a six-membered ring, the framework suffers considerable T−O−T angle distortions, from 2 to 15°, see Table 2. Furthermore, the two largest distortion values are found in the four-membered rings, which would lead to large energy penalty, because small rings are known to be very rigid.[17,18,26,32] The question is how this situation can be made more favorable.

The large distortions in both four-membered rings are overcome by the increase of the electrostatic interaction between the oxygen atoms of both rings and the $[ZnOZn]^{2+}$ cation. One observes that the distortions favors a better arrangement of these rings, creating a "boat-shape" ring configuration that increases the packing of the cation. This can be understood from the reduction of the T(6)−O−T(1), T(4)−O−T(5), and T(6)−O−T(1) angle values upon cationic exchange (see Table 2). This is also confirmed by the balanced interaction of both Zn cations with the oxygen atoms of the ring; see Table 2.

Interestingly, both positions 03 and 04 are the most favorable sites and have the same Al location within the ring. This indicates that such arrangement can either better accommodate the stress in the ring, as seen for the Zn(II) case,[26] or promote the electrostatic interaction between the extraframework cation and the framework oxygen atoms, as seen for both cations.

3.2.2. Eight-Membered Ring Family. This family corresponds to the three positions 05. A comparison between the formation reaction and the absolute energies [Table 1: entries 05(AlSiAl), 05(AlSiSiAl), and 05(AlSiSiSiAl)] indicates the Brønsted acid sites prefer to be formed in HO−Al−O−Si sequences. The most stable position for Brønsted acid sites in the eight-membered ring is the position 05(AlSiSiSiAl), in which both sites belong to the same four-membered ring (not shown here). This HO−Al−O−Si sequence preference seems to be a general trend, because the same result has been also found previously for six-membered ring positions.[26] Moreover, this trend confirms the suggestion from Derouane and co-workers[33] for the location of Al atoms in the zeolite framework.

As seen previously, taking into account only the absolute energy of the site ($E([ZnOZn]^{2+})$), the stability trend turns to be the following: position 05(AlSiSiSiAl) > position 05(AlSiAl) > position 05(AlSiSiAl). This result follows the same trend found for the six-membered rings. This generates the question: Why does such symmetrical arrangement of Al atoms stabilize the $[ZnOZn]^{2+}$ cation in the eight-membered ring?

First, both Zn cations are better stabilized by the electronic density of the framework oxygen atoms when these cations are placed on the same plane of the ring. As seen before, the average value for the Zn−O distance may show a possible trend. These values are 2.04 Å for 05(AlSiAl), 2.03 Å 05(AlSiSiAl), and 2.01 Å for 05(AlSiSiSiAl). These results show that in all cases both cations are located closer to the ring plane; therefore, all three eight-membered ring configurations stabilize similarly both Zn cations. However, since these rings are large, the cations can be better located within the ring plane, as seen from Figure 3. This may explain the best stability of the eight-membered family compared to that of the six-membered one.

Another factor is the accommodation of the framework stress after cation exchange. This stress has been assessed by measuring the changes in the T−O−T and O−T−O angles of the eight-membered ring. For instance, the O(3)−Al−O(1) and O(4)−T−O(2) angles are more acute due to the interaction with the $[ZnOZn]^{2+}$ site (see Table 3), which creates localized distortions in these rings. The energy penalty that would appear from these distortions could be minimized by sharing the stress among all ring links. This is better shown to occur for the 05(AlSiSiSiAl) and 05(AlSiAl) cases, which T−O−T angle values increase and decrease alternatively after the cation exchange; see Table 3. The same effect is not observed for the other configuration, which there is a localized distortion, see entries T8−O−T1, T1−O−T2, and T2−O−T3 in Table 3.

TABLE 3: Results for the Optimized Geometry of the Eight-Membered Ring Positions

	position 05					
Al distribution active site	AlSiAl		AlSiSiAl		AlSiSiSiAl	
	H^+	$[ZnOZn]^{+2}$	H^+	$[ZnOZn]^{+2}$	H^+	$[ZnOZn]^{+2}$
T(1)−O−T(2)	135.9	139.3	157.8	156.8	140.4	138.4
T(2)−O−T(3)	135.6	132.0	138.4	132.0	142.0	144.6
T(3)−O−T(4)	137.3	146.3	138.4	145.4	151.9	151.7
T(4)−O−T(5)	146.3	142.3	144.8	142.3	131.8	137.4
T(5)−O−T(6)	141.5	145.1	134.0	141.2	139.7	131.5
T(6)−O−T(7)	147.6	141.5	143.8	142.2	142.3	144.4
T(7)−O−T(8)	149.4	154.4	137.0	144.7	151.5	156.4
T(8)−O−T(1)	144.3	138.9	141.1	134.9	131.8	138.5
O(4)−Al−O(2)	94.1	90.6	98.0	93.4	105.4	90.7
O(1)−Al−O(3)	94.0	92.1	96.5	93.8	105.3	91.5
Zn(1)−O(1)		2.22		2.11		1.96
Zn(1)−O(3)		1.90		1.94		2.08
Zn(2)−O(2)		2.07		2.06		1.98
Zn(2)−O(4)		1.97		1.99		2.03
Zn(1)−O(5)		1.78		1.77		1.78
Zn(2)−O(5)		1.79		1.78		1.78
area (Å^2)	66.6π	66.8π	65.5π	64.9π	65.9π	67.9π

An interesting consequence of these distortions is the change in the eight-membered ring area. This has been calculated by assuming that the ring geometry could be approximated as having an ellipse form. The two semiaxis (*a* and *b*) values have been obtained by measuring the distances between T1-T5 and T3-T7 atoms in all three different configurations. The values for protonic and $[ZnOZn]^{2+}$ cases are shown in Table 3. The area increases upon cation exchange for the case of position 05(AlSiSiSiAl): it is almost constant for position 05(AlSiAl) but lessens for the last case. These results confirm that both Zn cations are siting almost on the ring plane in the case of position 05(AlSiSiSiAl).

Both electrostatic interaction and accommodation of the stress contribute for the stabilization of the 05(AlSiSiSiAl) configuration. Moreover, they seem to be not completely independent in this case. This does not occur for the other two cases. The position 05 (AlSiAl) is more stable than position 05(AlSiSiAl) because of the best minimization of the framework tension that occurs in the former case.

4. Conclusions

The location of the $[ZnOZn]^{2+}$ cluster in the chabazite zeolite has been studied by the periodical density functional method. Two Si atoms have been substituted by two Al atoms in the same D6R unit cell of the chabazite framework. This leads to different arrangements for Al pair in the six- and eight-membered ring configurations.

The cation is more stabilized when placed in the eight-membered ring. There are two factors playing a role in the stabilization of this site: the accommodation of the framework

stress and electrostatic interaction provided by the oxygen atoms of the framework.

The six-membered ring does not suffer extended distortions because the $[ZnOZn]^{2+}$ site sits out of the ring plane. However, the stability of the site is markedly influenced by the electrostatic interaction provided by the oxygen atoms of the framework due to the close proximity of both Zn^{2+} cations to the framework oxygen atoms.

Both mentioned factors are important for the stability of the $[ZnOZn]^{2+}$ site in eight-membered rings. However, accommodation of the framework stress seems to be the main cause of the different degrees of stabilization found within the eight-membered family. The location of Al atom within this large ring is the key factor that controls the flexibility, which minimizes this stress.

Acknowledgment. L.A.M.M. Barbosa thanks Eindhoven University of Technology (TUE, The Netherlands) for the computational time in the supercomputer facilities at SARA.

References and Notes

(1) Ono, Y. *Catal. Rev. Sci. Eng.* **1992**, *34*, 179.
(2) Frash, M. V.; van Santen, R. A. *Phys. Chem. Chem. Phys.* **2000**, *2*, 1085.
(3) Biscardi, J. A.; Meitzner, G. D.; Iglesia, E. *J. Catal.* **1998**, *179*, 192.
(4) Kumar, N.; Lindfors, L.-E. *Catal. Lett.* **1996**, *38*, 239.
(5) Nicolaides, C. P.; Sincadu, N. P.; Scurrel, M. S. *Catal. Today* **2002**, *71*, 429.
(6) Barbosa, L. A. M. M.; van Santen, R. A. *J. Mol. Catal. A* **2001**, *166*, 101.
(7) Laidlaw, P.; Bethell, D.; Brown, S. M.; Watson, G.; Willock, D. J.; Hutchings, G. J. *J. Mol. Catal. A* **2002**, *178*, 205.
(8) Penzien, J.; Müller, T. E.; Lercher, J. A. *Microporous Mesoporous Mater.* **2001**, *48*, 285.
(9) Kazansky, V. B.; Kustov, L. M.; Khodakov, A. Y. *Zeolites: Facts, Figures, Future*; Jacobs, P. A., van Santen, R. A., Eds.; Elsevier Science Publishers: Amsterdam, 1989; p 1173.
(10) Uvarova, E. B.; Kustov, L. M.; Lishchiner, I. I.; Malova, O. V.; Kazansky, V. B. *Stud. Surf. Sci. Catal.* **1997**, *105*, 1243.
(11) Kazansky, V. B.; Borovkov, V. Y.; Serykh, A. I.; van Santen, R. A.; Stobbelaar, P. J. *Phys. Chem. Chem. Phys.* **1999**, *1*, 2881.
(12) Kazansky, V. B.; Borovkov, V. Y.; Serykh, A. I.; van Santen, R. A.; Anderson, B. G. *Catal. Lett.* **2000**, *66*, 39.
(13) Kazansky, V. B.; Borovkov, V. Y.; Serykh, A. I.; van Santen, R. A.; Anderson, B. G. *Catal. Lett.* **2001**, *74*, 55.
(14) Boudart, M.; Garten R. L.; W. N. Delgass, W. N. *J. Phys. Chem.* **1969**, *73*, 2970.
(15) Valyon, J.; Hall, K. *J. Phys. Chem.* **1993**, *97*, 7054.
(16) Chen, H.-Y.; Sachtler, W. M. H. *Catal. Today* **1998**, *42*, 125.
(17) Barbosa, L. A. M. M.; Zhidomirov, G. M.; van Santen, R. A. *Catal. Lett.* **2001**, *77*, 55.
(18) Barbosa, L. A. M. M.; Zhidomirov, G. M.; van Santen, R. A. *Phys. Chem. Chem. Phys. A* **2000**, *2*, 3909.
(19) Yakovlev, A. L.; Shubin, A. A.; Zhidomirov, G. M.; van Santen, R. A. *Catal. Lett.* **2000**, *70*, 175.
(20) Kresse, G.; Furthmüller, J. *Comput. Mater. Sci.* **1996**, *6*, 15.
(21) Kresse, G.; Furthmüller, J. *Phys. Rev. B* **1996**, *54*, 169.
(22) Perdew, J.; Zunger, A. *Phys. Rev. B* **1981**, *23*, 8054.
(23) Perdew, J.; Wang, Y. *Phys. Rev. B* **1986**, *33*, 8800.
(24) Vanderbilt, D. *Phys. Rev. B* **1990**, *41*, 7892.
(25) Kresse, G.; Hafner, J. *J. Phys. Condens. Matter* **1994**, *6*, 8245.
(26) Barbosa, L. A. M. M.; van Santen, R. A. *J. Am. Chem. Soc.* **2001**, *123*, 4530.
(27) Demuth, T.; Hafner J.; Benco L.; Toulhoat, H. *J. Phys. Chem. B* **2000**, *104*, 4593.
(28) Jeanvoine, Y.; Ángyán, J. G.; Kresse, G.; Hafner, J. *J. Phys. Chem. B* **1998**, *102*, 7307.
(29) Brändle, M.; Sauer, J.; Dovesi, R.; Harrison, N. M. *J. Chem. Phys.* **1998**, *109*, 10379.
(30) Löwenstein, W. *Am. Miner.* **1942**, *39*, 92.
(31) Rozanska, X.; van Santen, R. A.; Hutschka, F.; Hafner, J. *J. Am. Chem. Soc.* **2001**, *123*, 7655.
(32) Hammonds, K. D.; Deng, H.; Heine, V.; Dove, M. T. *Phys. Rev. Lett.* **1997**, *78*, 3701.
(33) Derouane, E. G.; Fripiat, J. G. *Zeolites* **1985**, *5*, 165.